NOVEL ALGORITHM FOR ACTIVE SURFACE RECONSTRUCTION BY BAYESIAN CONSTRAINED SPECTRAL METHOD

Tomasz Sołtysiński*

* Institute of Precise and Biomedical Engineering, Department of Mechatronics, Warsaw University of Technology, Warsaw, Poland

solek@mchtr.pw.edu.pl

Abstract: Recently, an interesting application of spectral method was presented in which the penalized region growing and active surface techniques were driving segmentation of star-shaped objects in medical volume data obtained by noninvasive imaging techniques. We extend these techniques by application of Bayesian inference adapted to edge detection of noisy data instead of penalized region growing. The proposed algorithm offers a wide range of possible applications, from segmentation of highly noisy data to multimodal feature classification. We present application of the method to segmentation of ventricles in brain CT data affected by an aneurysm and disturbed by a significant noise. Scenarios of further improvements of Bayesian inference scheme applied to noise affected and multimodal data are provided in closing discussion.

Introduction

Segmentation of data from noninvasive medical imaging is widely used for computer-aided diagnostic and surgery. To achieve the most accurate or suitable segmentation, a number of advanced techniques has been developed [1]. Usually, most of these techniques use time consuming algorithms leading to the required segmented object or surface [2]. There is also a strong need for the methods that directly provide constraints for analytical models of shapes, surfaces and objects which can be further numerically processed by a virtual forces acting on their surfaces. This makes possible the prediction of deformation resulting from an invasive surgery or - monitoring the elastography of an object interacting with the surroundings within the body.

The process of reconstruction of a shape or surface may be effectively sped up by an application of spectral method based on fast Fourier transforms (FFT). This approach has the advantage of being rapid and accurate providing also the approximated surface that can be easily parametrized analytically by use of harmonic functions, splines or wavelets. An interesting application of such method, adapted for star-like objects has been proposed recently [3]. We partially follow this approach providing a different method for edge estimation based on Bayesian inference instead of volume penalization. This has the advantage of incorporating a wide range of the *a priori* knowledge coming from other modalities and global properties of structure. Throughout this paper we briefly describe the use of partial differential equations, we characterize the basics of Bayesian inference and its application into edge detection, we introduce the spectral method and the resulting novel algorithm as well as its application to CT data of brain ventricles. We discuss the results and the current limitations of the algorithm and provide some conclusions.

Methods

Application of PDE's in Shape or Surface Reconstruction

To recover an active surface from a data set we can approximate it by a set of shapes extracted from subsequent slices or describe the surface as a composition of the sum of an ensemble of 3D functions carrying details on different scales. The former approach is the subject of this study and serves as a direct basis for the latter. Let $g = g(\theta)$ be a noisy radial function defined in 2D spherical coordinates. The function g is called the polar edge map and can be estimated by a rough object's edge detection method like basic thresholding or watershed algorithm. The method is valid only for star-like objects with circumference described by g. To find function $f(\theta)$, the smooth representation of g, serving in fact as an approximation of the desired active shape, we need to apply a method directly revealing f by minimazing the energy functional:

$$E(f,g) = \mu \int_S Y(f,g) d\Omega_S + \int_S Z(f) d\Omega_S \qquad (1)$$

In the above eqution Y denotes the distance between the function f and polar edge map g, Z measures the reconstruction smoothness and μ is responsi-

ISSN: 1727-1983

ble for the tradeoff bewteen the faithfulness to the segmentation data and smoothness of the surface. $d\Omega_S$ is a differential shape element on the unit circle. Setting $Y(f,g) = (f(\theta) - g(\theta))^2$ and $Z(f) = \| \nabla \|^2$, where ∇ is the gradient operator the energy functional becomes

$$E(f,g) = \int_S \mu(f(\theta) - g(\theta))^2 d\Omega_S + \int_S \| \nabla \|^2 \, d\Omega_S \tag{2}$$

$E(f,g)$ can be further minimized over f by the usage of calculus of variation to determine an Euler-Lagrange equation for a stationary point of the above energy functional. This procedure yields the following equation:

$$\nabla^2 f - \mu(f-g) = 0 \tag{3}$$

This is an elliptic equation of Helmholtz type as is our case of spherical coordinates. Moving the g term to right hand side and relating it to a previously found value of f, called f_n the PDE can be expressed in linearized form:

$$\alpha \nabla^2 f_{n+1} - f_{n+1} = g_{f_n} \tag{4}$$

which can be easily solved by the fast spectral method, with $\alpha = 1/\mu$. The dependence of g_{f_n} on g and other data is the essence of our approach and is explained throughout next subsections.

Bayesian Constraint on Edge Map Determination

The most important contribution of this work is the bayesian method for edge map determination. The bayesian methodology provides the best choice among all others taking into account the risk associated with each one and their mutual relationship [4].

Let $P(E_i/I)$ denote the required probability of the most appriopriate edge in our existing data set. This is conditional probability as it depends on the content of I. $P(E_i/I)$ describes how much the given data point in I belongs to the edge E_i knowing the value of this point. It is intensity in our case and the knowledge we look for. Let $P(I/E_i)$ be a probability of how much the value or intensity of a point is depending on edge E_i. This term serves as a kernel. $P(E_i)$ is simply the probability of existence of the edge E_i among all other detected edges. Then the required probability can be found by solving the Bayes rule:

$$P(E_i/I) = \frac{P(I/E_i)P(E_i)}{P(I)} = \frac{P(I/E_i)P(E_i)}{\sum_i P(I/E_i)P(E_i)} \tag{5}$$

$P(I)$ is a sum of all probabilities $P(I/E_i)$ weighted by $P(E_i)$ and thus remaining constant. $P(I)$ is only a normalizing term and can be excluded from further analysis. The standard way of solving the equation is the maximization of the right hand side over the parameter E_i and then maximization of the found solution over all accesible data. The former procedure is known as *maximum likelihood* (*ML*) and the latter as *maximum-a-posteriori* (*MAP*). The $P(E_i)$ is a *prior* and we put our *a priori* knowledge inside it.

In practice we are estimating the $P(I/E_i)$ from the histogram of I. The histogram is shrank in such a way that each bin is equal to the edge size assuming that each expected edge covers the same number of intensity levels. Calculating the normalized probability over all edges E_i we are performing *ML* step and estimating the most probable edge in I. Then the *MAP* is done by searching for maximum over the data itself, and usually the first maximum in $P(I/E_i)$ is detected as an edge. The $P(E_i)$ is simply of constant value. Having this knowledge we can easily determine the position of edge in I even if the data is highly corrupted by noise.

Performing the classification of $P(E/I)$ we estimate G, which is bayesian constrained edge map. Calculating it for each θ_j we find the representation of rough polar edge map. This process is summarized by following equations:

$$G = classification(P(E/I)) \tag{6}$$

and

$$g(\theta) = G(\theta) \tag{7}$$

Fast Spectral Method

The spectral methods are widely used for all kind of problems that can be expanded into Fourier series. For the purpose of this study we adapt Cheong's method to solve the equation 3. We express the Laplacian operator ∇^2 on the unit circle:

$$\nabla^2 = \frac{1}{sin\theta} \frac{\delta}{\delta\theta} \left(sin\theta \frac{\delta}{\delta\theta} \right) \tag{8}$$

Both functions, f and g are defined on the computational grid (θ_i), where $\theta_i = \pi(j+0.5)/J$. J is the number of points along the longitude of unit circle's circumference high enough to engage all points covered by g. Each point in g may be now expressed by its discrete cosine transform (DCT) representation yielding:

$$g(\theta_i) = \sum_{n=0}^{J-1} g_n cosn\theta_i \tag{9}$$

with g_n being simply the coefficients of discrete cosine transform. Applying 8 into 3 we can write the equation 3 as an ordinary differential equation (ODE):

$$\frac{1}{sin\theta} \frac{\delta}{\delta\theta} \left(sin\theta \frac{\delta}{\delta\theta} f(\theta) \right) = \mu[f(\theta) - g(\theta)] \tag{10}$$

ISSN: 1727-1983

which yields an algebraic system of equations in Fourier space:

$$p_{n-2}f_{n-2} - p_n f_n + p_{n+2}f_{n+2} = \mu\left[\frac{1}{4}g_{n-2} - \frac{1}{2}g_n + \frac{1}{4}g_{n+2}\right] \quad (11)$$

where

$$p_{n-2} = \frac{(n-1)(n-2)+\mu}{4} \quad (12)$$

$$p_n = \frac{n^2+\mu}{2} \quad (13)$$

$$p_{n+2} = \frac{(n+1)(n+2)+\mu}{4} \quad (14)$$

after substitution of 9 into 10 and expressing f in the same way as g (eq.9). The index $n = 1,3,...,J-1$ for odd n and $n = 0,2,...,J-2$ for even n. The system of equation 11 may be now expressed as a double matrix equation:

$$\mathbf{B}_e\overline{f}_e = \mathbf{A}_e\overline{g}_e \quad (15)$$

$$\mathbf{B}_o\overline{f}_o = \mathbf{A}_o\overline{g}_o \quad (16)$$

with subscripts e for even and o for odd n, $\overline{f}$ and $\overline{g}$ denote the column vector of expansion coefficients of $f(\theta)$ and $g(\theta)$, respectively. **B** is a tridiagonal matrix containing the left hand side of equation 11 and **A** is tridiagonal matrix with constant coefficients along each diagonal corresponding to right hand side of 11.

The algorithm

The performance of shape reconstruction is done in two steps. Firstly, we analyze the data and classify the most probable edges according to given benchmarks. This is realized by bayesian procedure described previously. Secondly, the equation 4 is solved in an iterative way, and in the each step the right hand side term is updated by its current approximation obtained by inverse DCT (IDCT) from the cosine expansion coefficients derived from the residuals remaining after substraction of the rough edge map and currently found solution, obtained by IDCT from the vector f_n. The calculated set of expansion coefficients f_{n+1} serves for the reconstruction of f_i, the representation of g on the certain level of approximation i. This function carries the information about the structure of the real edge on given scale i. Summing all partial functions f_i we recover the required smooth approximation to g, recovering the most probable edge map.

Data

To test the algorithm we use the CT data, affected significantly by high level of noise. This circumstance introduces uncertain edge position and causes the poor quality of data. The adapted data set is publicly available on the web [5] and presents the brain with aneurysm. We are focused on brain cavities (ventricles) segmentation from the previously extracted data subset, covering the region of ventricles through 10 vertical slices. The structure in the image is hardly visible and nondetectable under 3σ level, where σ is standard deviation of all image pixels.

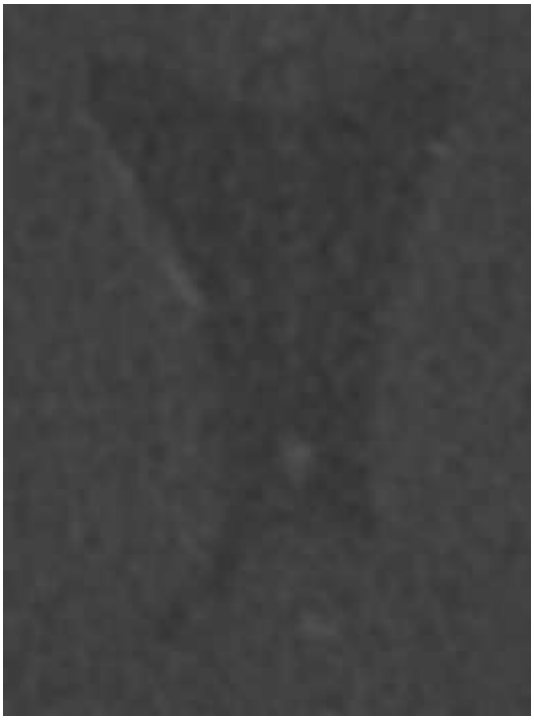

Figure 1: Raw data including the brain ventricles. High level of noise makes it hardly detectable and provides ill-posed edges.

Results

The results are presented through Figure 2 to 4. The noisy image of brain ventricles is composed of narrow range of 30 intensity levels. The effect of the algorithm's performance is shown in Figure 2. There are regions where the roughly eye-estimated detection is very good and some with rather high discrepancy, especially along vertical axis of the ventricles structure. This is due to some bright spots found over and below the ventricles which incorporate high gradients misinterpreted as a proper edge. The artefacts of this kind are hard to avoid in real noisy scans and disturb the bayesian edge detection. Fortunately, the spectral method smooths the required solution and much of this disturbance is removed from final region border, as shown on Figure 3. Through the next section we briefly discuss how to avoid such misinterpretation un-

ISSN: 1727-1983

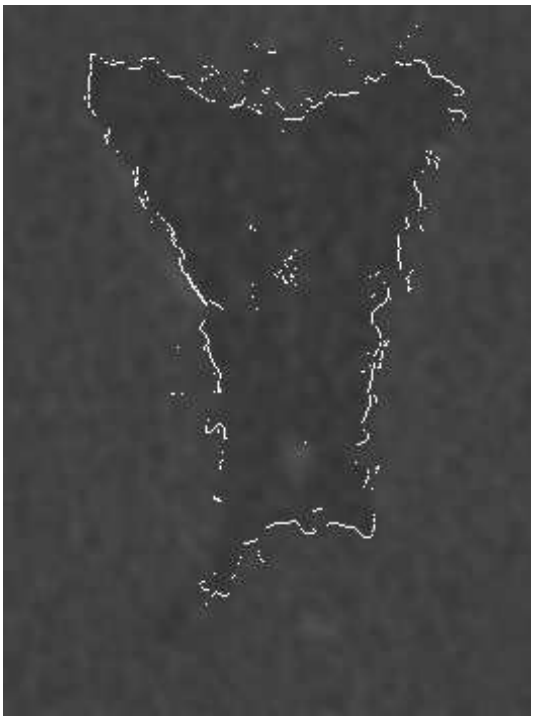

Figure 2: The Bayesian estimation of edge shape and position in the image data. Bright points mark all detected edges. The detection of an edge means the occurence of an edge of the highest probability. According to some distortions in the image some imperfections in the edge recognition are visible on the upper and lower part along the image vertical axis.

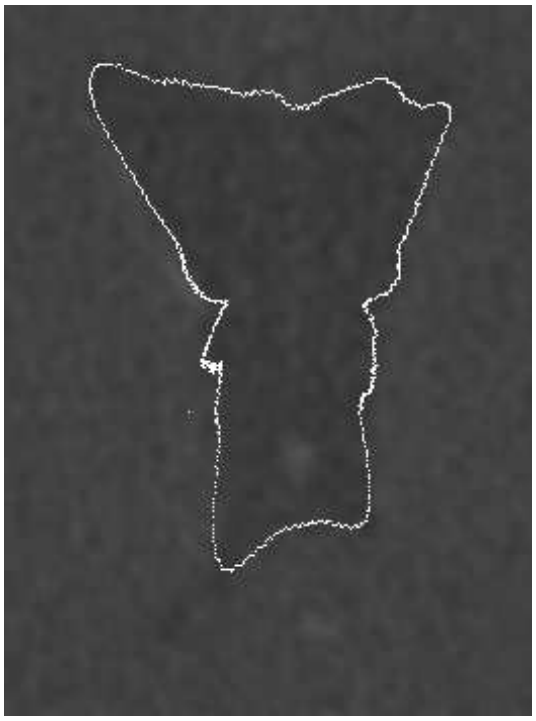

Figure 3: The segment border reconstructed by presented algorithm based on spectral method. The curve was recovered from Bayesian edge mark points shown on Figure 2.

der Bayesian inference. As one can notice from Figure 4 the bayesian constrained spectral segmentation provides smooth and very natural output. Traditional thresholding methods provide typical region with sharp and complicated edges, resembling its fractal nature. This artifact comes from noise which hides the real structure which is usually much more ordered in living macroscopic tissues. Thresholding bases on local properties in opposition to Bayesian constrained spectral method which reveals the entire shape at once taking advantage of all mark points.

The active surface of ventricles is composed of active shapes extracted from each slice and its example is presented on Figure 5. All shapes have been combined as a volume and rendered to show 3D structure of ventricles with the application of method described in [6]. The image shows hidden smooth natural representation of ill-posed fuzzy structure carried by data.

Discussion

It is clearly seen that the thresholding scheme reveals the border depending only on the local information, contained in the most neighbouring pixels while the Bayesian constrained spectral analysis recovers the border based on the total properties of the entire structure. The edge found by the thresholding scheme represents the real surface rather poorly introducing many local rich substractures. Although this can be decreased by means of sophisticated morphological analysis the Bayesian inference on edge determination naturally provides the desired shape or surface. It also highly supports the global analysis of the structure, providing the basis for elastography. This is due to the fact that the final shape or surface is composed of a number of less detailed curves or surfaces and each one can be further parametrized by base functions (splines, wavelets or harmonic functions) directly leading to an analytical model of surface that can be influenced by an external or internal force. The summation of partial shapes or surfaces on different levels of details also effectively supports the multiresolution properties of surfaces, that can be performed for some diagnostic reasons.

The Bayesian inference in application to edge detection can be further enhanced and developed. In the approach shown throughout this study we are maximizing only the ML step, limiting the MAP step to the detection of the first edge on given radius only. This can be more efficiently performed by maximizing MAP over a

ISSN: 1727-1983

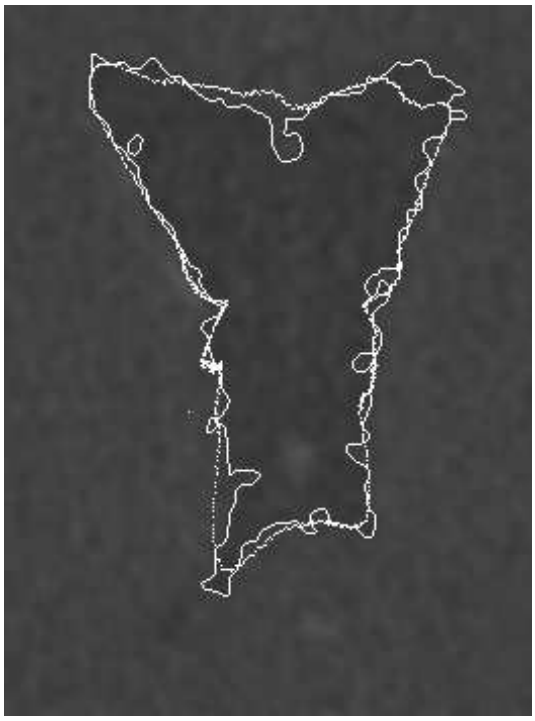

Figure 4: Comparison of Bayesian derived segmentation with that done by the best thresholding.

larger data set coming from neighboring radii or some predefined neighborhood. Further, the MAP maximization can be introduced by applying other modalities corresponding to a locally analyzed region in which the required edges are much more visible. Combining CT and PET is a good example of multimodal Bayesian inference to recover the edges in PET data. In PET the edges are almost invisible and additional information from CT, where they are easily detectable is necessary. Maximizing the MAP step is also a way to remove artifacts mentioned in section 3 (see 2 and 3). Increasing the data region for the MAP step or incorporating the information from edge filters into the MAP step can also increase the probability of right edge detection and decrease that of the fake one what leads to complete removal of all artifacts. Moreover, the proper choice of different nonuniformly distributed priors is going to significantly improve the algorithm's performance. This work is a subject of further research on the presented methods.

Conclusions

The new method presented here combines well-known and widely used methodologies, fast spectral method and Beyesian inference. Both ofer specific features, effectively supporting certain class of problems like segmentation and parametrization of moving

Figure 5: The final surface derived by Bayesian constrained spectral method applied to 10 slices independently.

shapes or surfaces that change their geometry in time. Although the method is limited to for radially described structures only, like liver, heart, some brain subsections, it is well suited for the analysis of noisy and disturbed data. Bayesian approach allows for more complex choice of priors and effective incorporation of any prior knowledge taken from other modalities as well as from the analysed data itself. Providing rapid algorithm this methodology is a promising direction of research for current and future applications.

References

[1] ROGOWSKA, J. Overview and fundamentals of medical image segmentation. In I.N. Bankman, editor, *Handbook of Medical Imaging, Processing and Analysis*, pages 69–86. Academic Press, 2000.

[2] MCINERNEY, T., TERZOPOULOS, D. Deformable models. In I.N. Bankman, editor, *Handbook of Medical Imaging, Processing and Analysis*, pages 127–146. Academic Press, 2000.

[3] LI, J. and HERO A.O. A fast spectral method for active 3d shape reconstruction. *Jour. of Math. Imaging and Vision*, 20:73–87, 2004.

[4] LAIDLAW, D.H., FLEISCHER, K.W., BARR, A.H. Partial volume segmentation with voxel histograms. In I.N. Bankman, editor, *Handbook of Medical Imaging, Processing and Analysis*, pages 195–214. Academic Press, 2000.

[5] THE VOLUME LIBRARY. Internet site address: http://www9.cs.fau.de/persons/roettger/library.

[6] SOLTYSINSKI, T. Multimodal visualization of volumes in noninvasive medical 3D imaging within idl environment. *Proc. of KBIB 2005, National Conference on Biomedical Engineering, in polish*, 2005.

ISSN: 1727-1983